

Cite this: *Mol. BioSyst.*, 2017,  
13, 1545

# Phosphorylation of a full length amyloid- $\beta$ peptide modulates its amyloid aggregation, cell binding and neurotoxic properties

Elaheh Jamasbi,<sup>a</sup> Frances Separovic,<sup>a</sup> Mohammed Akhter Hossain<sup>\*ab</sup> and  
Giuseppe Donato Ciccotosto<sup>id</sup><sup>\*c</sup>

Amyloid beta peptide (A $\beta$ ) is the major protein component of the amyloid plaques that are present in the brains of Alzheimer's disease (AD) patients. A $\beta$ 42 peptide is a known neurotoxic agent that binds to neurons and, under specific aggregation conditions, triggers cell death. A $\beta$  peptide can undergo specific amino acid posttranslational modifications, such as phosphorylation, that are important for modulating its proteolytic degradation, aggregation, binding to lipid membranes and neurotoxic functions. Peptides phosphorylated at serine 8 in full-length A $\beta$ 42 (pA $\beta$ 42) were synthesised and compared to native A $\beta$ 42 peptide. Their secondary structures, aggregation properties and interactions with plasma membranes of primary cortical neurons were investigated. The results revealed that pA $\beta$ 42 has increased  $\beta$ -sheet formation with rapid amyloid formation in a synthetic lipid environment, which was associated with increased cellular binding but concomitant diminished neurotoxicity. Our data support the notion that phosphorylation of A $\beta$ 42 promotes the formation of amyloid plaques in the brain, which lack the neurotoxic properties associated with oligomeric species causing pathogenesis in AD.

Received 27th April 2017,  
Accepted 29th May 2017

DOI: 10.1039/c7mb00249a

rsc.li/molecular-biosystems

## Introduction

Alzheimer's disease (AD) is a progressive neurodegenerative disorder that has a devastating impact on our aging population as it causes clinical memory loss, confusion, cognitive deficits and brain atrophy.<sup>1</sup> A major pathological hallmark of AD is the extracellular accumulation of amyloid- $\beta$  (A $\beta$ ) peptide as insoluble amyloid plaques, an event that precedes the formation of the intraneuronal neurofibrillary tangles (composed of hyperphosphorylated tau) in the brain which lead to significant synaptic damage and neuronal cell death.<sup>1,2</sup> Thus, while phosphorylation of the tau protein dramatically alters its properties, little is known about how phosphorylation of A $\beta$  modulates its biological properties. A full-length A $\beta$  peptide has 42 amino acids and there are three potential amino acid phosphorylation sites – serine at positions 8 and 26 and tyrosine at position 10.<sup>3</sup> Phosphorylated A $\beta$  (pA $\beta$ ) has been detected in brain samples from APP transgenic mice<sup>4,5</sup> and in human brain,<sup>5</sup> brain plaques and blood samples from patients diagnosed with AD,<sup>6</sup> while

human cerebrospinal fluid has been shown to exhibit A $\beta$  phosphorylating activity.<sup>7</sup> Further analysis revealed that pA $\beta$  accumulation in the parenchyma and vasculature deposits was mainly found in late-stage AD brains.<sup>8</sup> In addition, a positive correlation between the soluble pA $\beta$  concentration and angiotensin converting enzyme activity in the parahippocampal cortex, but not in the midfrontal cortex, was found, suggesting that a positive feedback mechanism exists between pA $\beta$  and the enzyme.<sup>8</sup> Phosphorylation also decreased A $\beta$  proteolytic degradation and clearance by microglial cells.<sup>9</sup> Taken together, phosphorylation of A $\beta$  therefore has a number of important roles in promoting AD pathogenesis, including promoting aggregation and decreasing its proteolytic clearance.

The ability of A $\beta$  to bind lipids and form amyloid plaques indicates that its interaction with neuronal membranes is a key event for its aggregation into toxic species to induce neurotoxicity.<sup>10–12</sup> Thus, it is important to understand whether posttranslational modifications of A $\beta$  can modulate its interaction with lipid membranes, lead to the peptide acquiring cytotoxic properties and cause cell death. Since phospholipids and cholesterol are the main components of membranes,<sup>13</sup> the interactions of A $\beta$  peptide with membrane lipids and lipid mimetic compounds were studied. However, in order to further understand the effect of phosphorylation, we chemically synthesised full-length native A $\beta$ 42 and pA $\beta$ 42 with the serine phosphorylated (pSer) at position 8 and examined their interactions with lipid

<sup>a</sup> School of Chemistry and Bio21 Institute, The University of Melbourne, VIC 3010, Australia

<sup>b</sup> The Florey Institute of Neuroscience and Mental Health, The University of Melbourne, VIC 3010, Australia. E-mail: akhter.hossain@florey.edu.au

<sup>c</sup> Department of Pathology, The University of Melbourne, VIC 3010, Australia. E-mail: jicco@unimelb.edu.au



membranes using both a synthetic model membrane and mouse primary cortical cultures.

## Results

### Synthesis of full-length phosphorylated A $\beta$ 42 peptides

We determined the optimised conditions for synthesising and purifying A $\beta$ 42 and pA $\beta$ 42 peptides. For the preparation of pA $\beta$ 42 peptide, while the whole chain was synthesised using 5 minutes of microwave coupling at 86 °C, some residues were coupled at room temperature for extended periods of time (up to 1 h). This was to minimise de-phosphorylation, racemization or aspartimide formation, particularly for the coupling of pSer, aspartic acid, histidine or cysteine amino acids. The amino acids were assembled on commercially available alanine loaded solid phase Wang resin. The advantage of this resin is that it swells efficiently in the solvent used for coupling and phosphorylation. We determined the optimal conditions for the elution solvent (B: Isp: ACN: Milli-Q = 40:40:20; A: 0.1 M ammonium acetate buffer pH 9.2; gradient of B: 20–50% in 30 min) and used a high temperature (50 °C) to purify the A $\beta$ 42 and pA $\beta$ 42 peptides because of their very hydrophobic and aggregating properties. For the synthesis of the AlexaFluor labelled peptides, the serine residue at position 26 was replaced with a cysteine residue using a previously reported in-house procedure.<sup>14</sup> Chromatograms and mass spectra analyses are shown in Fig. 1.

### Amyloid aggregation formation of pA $\beta$ 42 in a lipid environment

Aggregation of A $\beta$ 42 and pA $\beta$ 42 was detected using a ThT fluorescence assay, which is routinely used for the identification and quantification of amyloidogenic  $\beta$ -sheet structural formation *in vitro*.<sup>15</sup> The ThT fluorescence profile of the pA $\beta$ 42 peptide was similar to that of the native A $\beta$ 42 peptide when suspended in PBS buffer only, displaying the typical initial lag phase and then undergoing rapid aggregation and reaching maximal fluorescence

at around 12 h (Fig. 2A). In the presence of POPS/POPC large unilamellar vesicles (LUVs), the ThT fluorescence intensity for the pA $\beta$ 42 peptide showed a slower aggregation profile and plateauing at 12 h again, while the ThT fluorescence intensity was at least double that of the native A $\beta$ 42 peptide (Fig. 2B). The inclusion of cholesterol in the POPS/POPC LUVs (POPS/POPC/Chol) resulted in initial rapid aggregation of the pA $\beta$ 42 at  $t = 0$  and slow and consistent aggregation over the 24 h incubation period, and the ThT fluorescence intensity was again at least double that of the native A $\beta$ 42 peptide over the whole incubation period (Fig. 2C).

### Secondary structure of pA $\beta$ 42 in a lipid environment

CD spectroscopy analysis was done to determine whether the secondary structure and folding properties of the phosphorylated A $\beta$ 42 peptide were modified in a PBS buffer environment and in the presence of synthetic lipid membrane model systems (Fig. 3). The results showed that the A $\beta$ 42 peptide in PBS buffer was mainly unstructured (Fig. 3A) while pA $\beta$ 42 adopted more  $\beta$ -sheet configuration (higher intensity  $\sim$ 200 nm and less intensity near  $\sim$ 215 nm) and random coil configuration (Fig. 3B). The addition of POPS/POPC LUVs to these peptides resulted in a changed confirmation for both peptides. For A $\beta$ 42, there was a small increase in the  $\beta$ -sheet structure while the addition of POPS/POPC/Chol LUVs led to a much higher intensity of random coil structure (Fig. 3A). In contrast, the addition of the POPS/POPC LUVs had only a small effect on pA $\beta$ 42 conformation showing some extended  $\beta$ -sheet structure but the presence of cholesterol in POPS/POPC/Chol LUVs had little effect on the secondary structure, which may be due to the faster aggregation or stronger interaction of this modified peptide with model membranes.

### Toxicity and cell binding properties of phosphorylated A $\beta$ 42

Having confirmed that the secondary structure and amyloid formation properties of pA $\beta$ 42 differed from the native A $\beta$ 42,

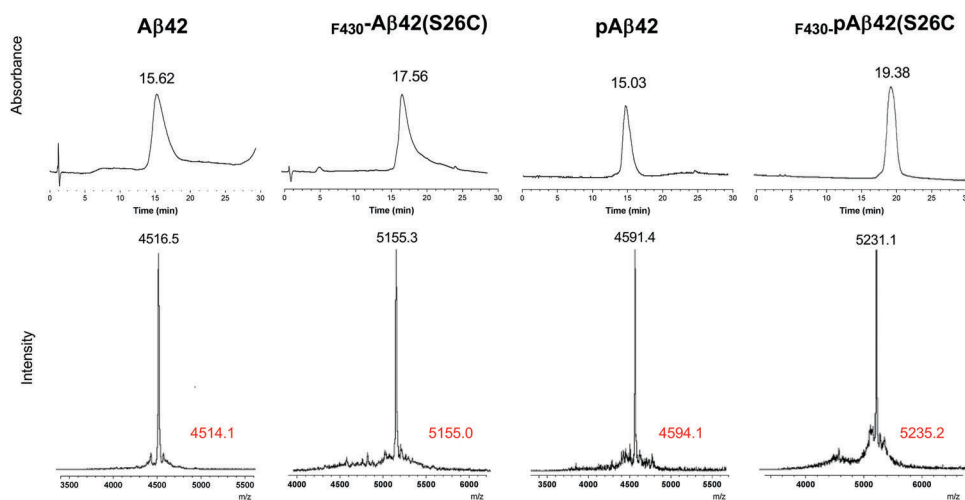


Fig. 1 Characterisation of purified synthesised A $\beta$ 42 peptides by chromatographic analysis. RP-HPLC (top panel) displaying peak elution times and MALDI TOF MS trace analysis (bottom panel) displaying calculated (black) and observed (red) mass values for each peptide synthesised.



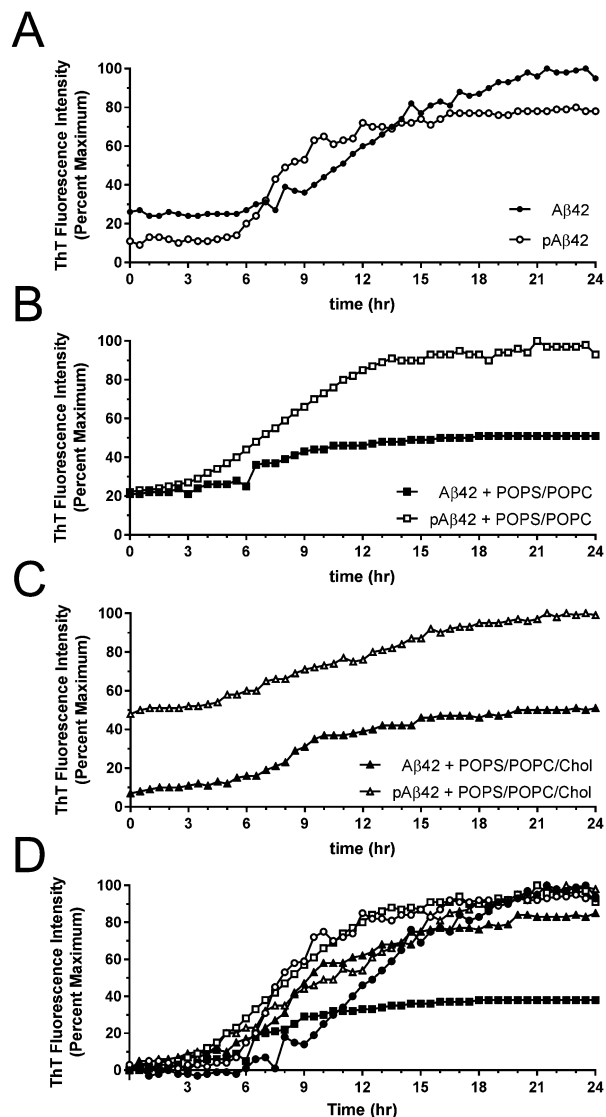


Fig. 2 Detection of amyloid structures by Thioflavin T (ThT) assay. Synthetically prepared A $\beta$ 42 (filled symbols) and pA $\beta$ 42 (open symbols) peptides (10  $\mu$ M) were analysed in the presence of (A) PBS buffer only (circles), (B) PBS buffer containing POPC/POPS LUVs (squares), and (C) PBS buffer containing POPC/POPS/Chol (triangles), at a peptide : lipid ratio of 1 : 30. The data were normalised to the maximum ThT level in the respective panels and (D)  $t = 0$  subtracted. Traces are representative of 3 different experiments.

we then tested the toxicity of these peptides in primary mouse cortical cultures. As expected, treating the cortical cultures for 4 days with native A $\beta$ 42 induced a significant reduction in cell viability at 15  $\mu$ M (Fig. 4). By contrast, pA $\beta$ 42 displayed no neurotoxicity at the same concentration (Fig. 4).

Since A $\beta$  neurotoxicity is associated with neuronal cell binding,<sup>11,16,17</sup> we examined whether the non-toxic nature of pA $\beta$ 42 may be due to an altered cell binding characteristic. This experiment was performed using F<sub>430</sub>-A $\beta$ 42(S26C) and F<sub>430</sub>-pA $\beta$ 42(S26C) labelled peptides at a subtoxic concentration (5  $\mu$ M). The labelled peptides were added to the primary cortical cultures for 24 h and cell binding was examined histologically using identical microscope and image acquisition settings (Fig. 5).

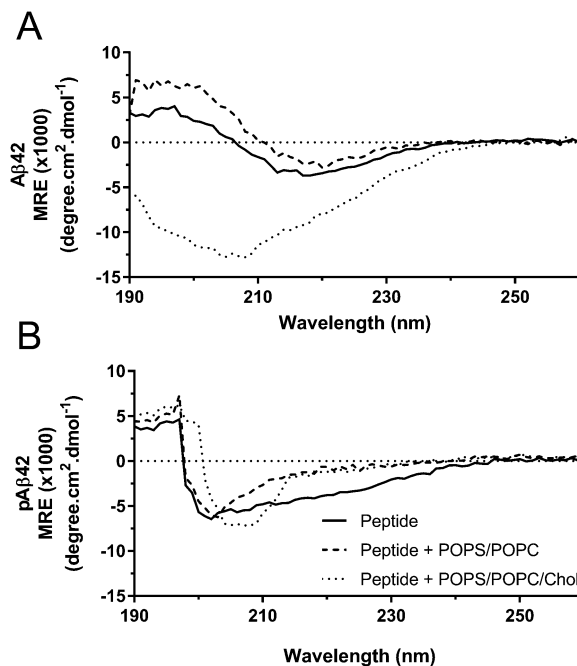


Fig. 3 The secondary structure of the synthesised A $\beta$  peptides was determined by CD spectral analysis. The CD spectral traces for (A) A $\beta$ 42 and (B) pA $\beta$ 42 peptides (10  $\mu$ M) were compared in solutions containing PBS buffer only (solid black line), PBS buffer containing POPC/POPS LUVs (long dashed black line), and PBS buffer containing POPC/POPS/Chol LUVs (dotted black line) at a peptide : lipid ratio of 1 : 30. Traces are representative of 3 different experiments.

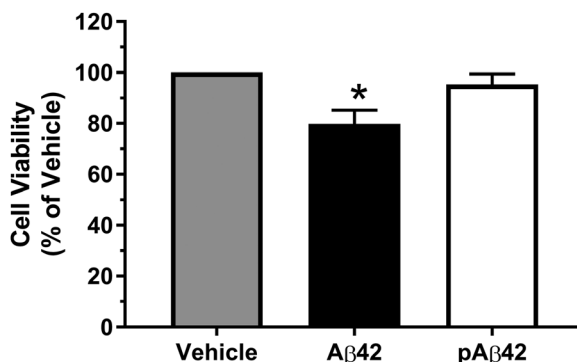


Fig. 4 Neurotoxicity of the synthesised A $\beta$ 42 and pA $\beta$ 42 peptides. Primary cortical neurons were grown at a density of 150 000 cells per  $\text{cm}^2$  for 6 days *in vitro* and the viability of these neuronal cultures was determined following 15  $\mu$ M peptide treatment for 96 h by CCK assay. The data were normalised and expressed as a percentage of the vehicle treated cultures. The results are mean  $\pm$  SEM. Statistical comparison between vehicle and treatment groups was done using the Students *t*-test. \*,  $p > 0.05$  vs. vehicle treated cells. Experiments were done in triplicate and repeated 3 times.

As expected, the native F<sub>430</sub>-A $\beta$ 42(S36C) peptide bound to the extracellular structures of the neuron in a punctate matter, as described previously<sup>11,16,17</sup> (Fig. 5A), while the F<sub>430</sub>-pA $\beta$ 42(S36C) peptide similarly bound to the plasma membrane surface of neuronal cell structures (Fig. 5B). The amount of cell surface binding was quantitated by identifying neuronal cell structures using an anti-Tau antibody, and the cell images were imported



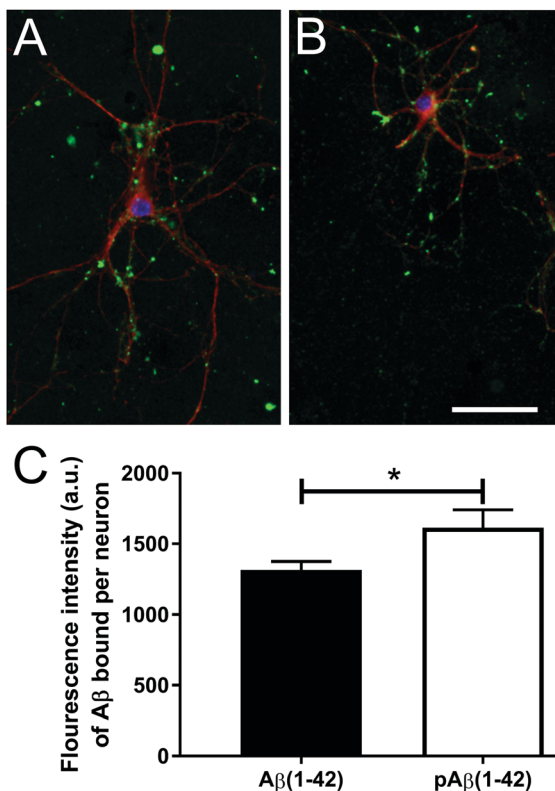


Fig. 5 Quantitation of A $\beta$  binding to cortical neurons. Neurons at 6DIV (150 000 cells per cm<sup>2</sup>) were treated for 24 h with 5  $\mu$ M of: (A) F<sub>430</sub>-A $\beta$ <sub>42</sub>(S26C) and (B) F<sub>430</sub>-pA $\beta$ <sub>42</sub>(S26C) (green); and (C) The amount of F<sub>430</sub>-A $\beta$  peptide binding to neurons was determined by histological analysis, as described in the Experimental section, and the calculated cell fluorescence intensity is graphed. Neurons were co-stained for Tau (red) and nucleus using DAPI (blue).  $N = 3$ . The results are mean  $\pm$  SEM. \*,  $p < 0.05$  vs. F<sub>430</sub>-A $\beta$ <sub>42</sub>(S26C) treated cells.

into an image analysis software program. The regions of interest around the neuronal cellular structures were identified and the fluorescence intensity levels of the A $\beta$  bound peptide molecules (*i.e.*, green channel) were measured, background regions subtracted and adjustments made to account for the number of neurons per image. The results show that the F<sub>430</sub>-pA $\beta$ <sub>42</sub>(S36C) peptide had a significantly higher fluorescence intensity compared to the native F<sub>430</sub>-A $\beta$ <sub>42</sub>(S36C) peptide (Fig. 5C).

## Discussion

This study reveals that posttranslational phosphorylation at Ser8 of full-length A $\beta$ <sub>42</sub> causes significant changes to its biophysical, neurotoxic and neuron cell binding properties. This is the first report using in-house peptide chemistry to synthesise a *bona fide* full-length peptide with site specific phosphorylation at Ser8 (pA $\beta$ <sub>42</sub> peptide). One of the major challenges of investigating the A $\beta$  peptide is its synthesis and purification, since the full-length A $\beta$ <sub>42</sub> peptide is very hydrophobic and, therefore, known as a very “difficult peptide” to make.<sup>18</sup> The major challenges associated with the synthesis of this peptide are due to its high content of hydrophobic residues that are present in the C-terminal sequence,

which makes solid phase synthesis of this peptide very challenging even without additional posttranslational modifications to specific amino acids.<sup>19,20</sup> Previous reports have investigated shorter A $\beta$  peptide sequences with phosphorylation at Ser8, pA $\beta$ (1-16)<sup>21</sup> and pA $\beta$ (1-40),<sup>5,9,22</sup> and Ser26 pA $\beta$ (1-40),<sup>23</sup> which were purchased from commercial suppliers. Alternatively, phosphorylated A $\beta$  peptides were prepared by incubating synthetic A $\beta$  peptides with enzymes, such as protein kinase A,<sup>5</sup> which readily phosphorylated S8 in A $\beta$ <sub>40</sub>, and human cdc2 kinase,<sup>24</sup> which bound to and induced phosphorylation purportedly at Ser26 for the A $\beta$ <sub>25-35</sub>, A $\beta$ <sub>40</sub> and A $\beta$ <sub>42</sub> peptides. We now provide the optimised conditions for successfully chemically synthesising and purifying full-length pA $\beta$ <sub>42</sub> peptides, as well as preparing F<sub>430</sub>-A $\beta$ <sub>42</sub>(S26C) peptides with greater than 96% purity.

The post-translational modifications of A $\beta$  peptide that are responsible for alterations to its secondary structure and aggregation propensity, particularly upon interaction with a lipid membrane, are contributing factors to the development of this AD pathogenesis. Our findings reveal that the pA $\beta$ <sub>42</sub> peptide aggregated in a similar manner to its native A $\beta$ <sub>42</sub> peptide in an aqueous environment, but in the presence of phospholipid POPS/POPC LUVs or POPS/POPC/Chol LUVs, the pA $\beta$ <sub>42</sub> peptide aggregated more rapidly and to a much higher extent compared to the native peptide. These results are in agreement with the pA $\beta$ <sub>40</sub>(S8) peptide, which also displayed a similar higher rate and amount of ThT reactive aggregate material compared to the native A $\beta$ <sub>40</sub> peptide<sup>5,22</sup> while aggregation of pA $\beta$ <sub>40</sub>(S26)<sup>23</sup> remained largely unchanged with only a slight increase in ThT absorbance after 30 h of incubation in a lipid-free model experiment. This increased aggregation of pA $\beta$ <sub>42</sub> was confirmed by the CD spectroscopy data, which revealed increased  $\beta$ -sheet formation in the presence of POPS/POPC/Chol LUVs (Fig. 3). Phosphorylation at Ser8 for A $\beta$ <sub>40</sub> led to the characteristic pattern of extended  $\beta$ -sheet structure only when it was allowed to aggregate for at least 2 h while in its monomeric state.<sup>5</sup> We and others show that pA $\beta$  is largely in a disordered state.<sup>5,22,23</sup> The combined *in vitro* data suggest that a lipid environment is an important parameter for the promotion and formation of amyloid structures for the A $\beta$  peptide.

We have previously shown that A $\beta$  peptide binding to neuronal cultures is a key determinant for inducing cell toxicity, with the notable key exception of the D-handed peptide, which while binding to neurons in culture was not toxic.<sup>11,16,17,25,26</sup> We observed a higher level of F<sub>430</sub>-pA $\beta$ <sub>42</sub>(S26C) binding compared to the F<sub>430</sub>-A $\beta$ <sub>42</sub>(S26C) peptide, which may be explained by the CD (Fig. 3) and ThT (Fig. 2) results, which showed that the pA $\beta$ <sub>42</sub> peptide had a higher propensity to aggregate and bind to model plasma membranes. The higher cell binding for F<sub>430</sub>-pA $\beta$ <sub>42</sub>(S26C) did not translate into increased cell toxicity (Fig. 4); rather, we saw diminished toxicity of the pA $\beta$ <sub>42</sub> peptide in our primary cortical cell culture model. Our results are in agreement with the results found for the p(S26)A $\beta$ <sub>40</sub> peptide, which also was not toxic to mouse primary cortical cultures.<sup>23</sup> However, the same laboratory found that the p(S8)A $\beta$ <sub>40</sub> peptide was toxic to human iPSC-derived neurons and p(S26)A $\beta$ <sub>40</sub> was toxic to both human neuroblastoma cells and iPSC-derived



neuronal cultures.<sup>27</sup> In addition, an *in vivo Drosophila* model, where a pseudo phosphorylated A $\beta$  was prepared with an S8D mutation, was found to strongly promote age-dependent degeneration of the photoreceptor cells in the eye of the *Drosophila* compared to native A $\beta$ .<sup>5</sup> Taken together, our results support the notion that phosphorylation of A $\beta$  promotes its rapid aggregation into non-toxic amyloid structures that are readily found on the extracellular membrane structures in the brain and represent the pathological hallmark for AD diagnosis.

## Conclusion

Synthetic preparation of a full-length A $\beta$ 42 peptide incorporating a phosphorylated Ser8 amino acid was found to promote aggregation into non-toxic amyloid structures, especially when in contact with a lipid membrane. Our results reveal that pA $\beta$ 42 has increased  $\beta$ -sheet formation with rapid amyloid formation in a model phospholipid membrane environment, which is associated with increased cellular binding but concomitant diminished neurotoxicity. The observations that the aggregation of A $\beta$  was substantially increased in the presence of pA $\beta$  seeds (*i.e.*: containing preformed oligomeric nuclei)<sup>5</sup> and that pA $\beta$  is mainly found in late-stage AD brains<sup>8</sup> in combination with our own cell binding data support the notion that the posttranslational phosphorylation of A $\beta$ 42 is an important event that promotes amyloid plaque formation in the brain, which lacks the neurotoxic properties associated with oligomeric species causing pathogenesis in AD.

## Experimental

### Materials

All chemicals and solvents were obtained from Sigma-Aldrich (Sydney, Australia) unless otherwise stated.

### Peptide synthesis

The A $\beta$ 42 and pA $\beta$ 42 peptides were synthesized using previously reported in-house procedures for peptide synthesis,<sup>14</sup> but a number of modifications and optimisation steps were required to achieve high levels of purity and yields. The peptides were synthesised using the Fmoc/*t*Bu solid phase strategy with microwave irradiation at 86 °C on a CEM Liberty synthesizer. The histidine, cysteine in the A $\beta$ 42 peptides and phosphoserine in the pA $\beta$ 42 peptides were coupled without microwaving. Fmoc protected amino acids were used for peptide synthesis (GL Biochem, China). Peptides were cleaved using trifluoroacetic acid (TFA), anisole, triisopropylsilane, and Milli-Q water (94 : 3 : 2 : 1) for the A $\beta$ 42 peptide; and TFA, anisole, triisopropylsilane, Milli-Q water, and thioanisole (90 : 2.5 : 2.5 : 2.5 : 2.5) for the pA $\beta$ 42 peptide. The crude peptides, except pA $\beta$ 42, were purified by RP-HPLC using a Phenomenex C4 column (particle size 5  $\mu$ m, 4.6  $\times$  150 mm), with a gradient of 10–90% acetonitrile (0.1% TFA) in 30 min. The pA $\beta$ 42 peptides were purified using isopropanol : acetonitrile : Milli-Q water at a ratio of 40 : 40 : 20 and with 0.1 M ammonium acetate buffer of pH 9.2 with a gradient of 20–50% in 30 min. The purity (96 and 98%) and yields (18 and 14%, calculated from

the crude starting material) were determined for A $\beta$ 42 and pA $\beta$ 42, respectively.

To prepare the fluorescently labelled A $\beta$  peptides, the serine residue (S) at position 26 in the peptide sequence was replaced with a cysteine residue (C). These A $\beta$ 42(S26C) and pA $\beta$ 42(S26C) peptides were synthesized and labelled with AlexaFluor 430 as NHS ester forms (Invitrogen, Sydney, Australia) using thiol-maleimide conjugation chemistry.<sup>14</sup> The coupling reaction between NHS-AlexaFluor 430 (1.4  $\mu$ mol, 1 mg) and *N*-(2-aminoethyl) maleimide (1.68  $\mu$ mol, 0.43 mg) was performed in the presence of *N,N*-diisopropylethylamine (2.68  $\mu$ mol, 0.05  $\mu$ l) in dimethylformamide. Mal-AlexaFluor was used to react with the side chain of the cysteine residue. The final A $\beta$ -AlexaFluor labelled peptides (termed F<sub>430</sub>-A $\beta$ 42(S26C) and F<sub>430</sub>-pA $\beta$ 42(S26C), respectively; Fig. 1) were purified using the same conditions as described for the unlabelled peptide. For F<sub>430</sub>-A $\beta$ 42 and F<sub>430</sub>-pA $\beta$ 42, respectively, the purities were 97 and 99% and the yields were 43 and 32% (calculated from purified A $\beta$ 42(S26C) peptides as the starting material).

### Peptide preparation

Lyophilised peptides were prepared by dissolving the peptides in a sequence of buffers at a ratio of 2 : 7 : 1 v/v. 20 mM NaOH was added to the peptide and vortexed and sonicated in an ice chilled water bath for 15 min to fully solubilise the peptide. Milli-Q water and 10 $\times$  PBS (2.7 mM KCl, 1.5 mM KH<sub>2</sub>PO<sub>4</sub>, 138 mM NaCl, 8 mM Na<sub>2</sub>HPO<sub>4</sub>, at pH 7.4) were added, the solubilised peptide was spun in a benchtop centrifuge at 16 000 g for 5 min (to remove amorphous aggregates) and the supernatant was transferred to a clean tube and stored on ice until used (typically within 1 h of its preparation). The final A $\beta$ 42 peptide concentrations were determined by UV absorption spectroscopy using the molar extinction coefficient of 75887 M<sup>-1</sup> cm<sup>-1</sup> at 214 nm.

### Preparation of model lipid membranes

Multilamellar vesicles were prepared using previously reported in-house procedures with slight modifications.<sup>10,17</sup> Briefly, phospholipids were sourced from Avanti Polar Lipids (Alabaster, USA) and desired amounts of 1-palmitoyl-2-oleoylphosphatidylcholine (POPC) and 1-palmitoyl-2-oleoyl-*sn*-glycero-3-phospho-L-serine (POPS) were combined together (POPC/POPS) at a 1 : 1 (w/w) ratio or with cholesterol (POPC/POPS/Chol) at a 1 : 1 : 1 (w/w) ratio and dissolved in a solution of chloroform and methanol at a 3 : 1 (v/v) ratio and the organic solvents were evaporated under vacuum to obtain a lipid film. The lipid film was placed under vacuum overnight to evaporate residual organic solvents. The dried film was resuspended in Milli-Q water, homogenised and extruded through a polycarbonate Whatman Nuclepore membrane (100 nm pore size) in 10 mM phosphate buffer pH 7.4 to produce large unilamellar vesicles (LUVs).

### Thioflavin T assay

Thioflavin T (ThT) fluorescence was used to monitor the presence of  $\beta$ -sheet amyloidogenic structures of the A $\beta$  peptides. ThT binds to aggregated A $\beta$  peptides, which causes an increase in ThT fluorescence, as measured by excitation at 440 nm and



emission at 482 nm. Briefly, A $\beta$ 42 and pA $\beta$ 42 peptides were prepared at 10  $\mu$ M in the presence of 20  $\mu$ M ThT in a 96 well microplate and incubated at 37 °C with orbital shaking at 700 rpm using a FLUOstar Omega plate reader (BMG Labtech, Melbourne, Australia) with 30 min readings taken over a 24 h period. The ThT assay was performed with 10  $\mu$ M A $\beta$  peptides in PBS buffer only (phosphate buffer, pH 7.4 and 1 mM NaCl), as well as in the presence of POPS/POPC LUVs and POPS/POPC/Chol LUVs at a peptide:lipid molar ratio of 1:30. All experimental combinations were performed at the same time.

### CD spectroscopy

The peptide secondary structure and conformational changes upon the addition of LUV lipid systems were studied using circular dichroism (CD) spectroscopy. CD traces were acquired at room temperature using a Chirascan-plus instrument, a 1 cm quartz cuvette and instrument settings of 1 nm step size, 1 nm bandwidth and a wavelength range of 190 to 260 nm. CD measurements were performed with 10  $\mu$ M A $\beta$  peptides in PBS buffer only, as well as in the presence of the prepared LUVs and LUVs plus cholesterol at a peptide:lipid molar ratio of 1:30. All the experimental combinations were performed on the same day.

### Primary neuronal cultures

Male and female 14-day-old embryonic mice were taken from pregnant female mice and used to prepare cortical neuronal cultures under sterile conditions, as described previously.<sup>13</sup> The mice were provided by the University of Melbourne, School of Biomedicine, Animal House Facility. These procedures were approved by a local institutional Animal Ethics Committee. Mouse cortical neuronal cultures were prepared under sterile conditions, as described previously,<sup>16</sup> and approved by a local institutional Ethics committee. Briefly, embryonic day 14 C57/BL6 mice cortices were removed, dissected free of meninges, and dissociated in 0.025% (w/v) trypsin in Krebs buffer. The dissociated cells were triturated using a filter-plugged fine pipette tip, pelleted, resuspended in plating media (minimum Eagle's media containing 10% fetal calf serum and 5% horse serum) and counted. Cortical neuronal cells were seeded at 150 000 cells per cm<sup>2</sup> for 2 h, then the plating media was replaced with freshly prepared neurobasal media containing B27 supplements, gentamicin, and 0.5 mM glutamine (NB/27). All the tissue culture reagents were purchased from Invitrogen, Melbourne, Australia, unless otherwise stated. Cells were seeded onto poly-D-lysine treated 48 well plates for cell viability assays, and onto 12 mm glass coverslips (placed in 24 well plates) for histological analysis. All cultures were maintained in a humidified incubator set at 37 °C supplemented with 5% CO<sub>2</sub>. This method resulted in cultures highly enriched for neurons (>95% purity) with minimal astrocyte and microglial contamination.

### Cell viability assays

The neuronal cells were allowed to mature for 6 days in culture before A $\beta$  treatment was commenced. Freshly prepared soluble A $\beta$  stock solutions were diluted to a final concentration of

15  $\mu$ M in freshly prepared neurobasal medium containing B27 supplements (minus antioxidants) and then added to the neuronal cells for 4 days of treatment in the 37 °C incubator. Cell viability was quantitated using the CCK8-assay kit (Dojindo, Auspep, Melbourne, Australia) as previously described.<sup>25</sup> The data were normalized and calculated as a percentage of vehicle-treated cells.

### Fluorescence histochemistry

The neuronal cells were allowed to mature for 6 days in culture before A $\beta$  treatment was commenced. Freshly prepared soluble F<sub>430</sub>-A $\beta$ 42(S26C) and F<sub>430</sub>-pA $\beta$ 42(S26C) stock solutions were diluted to a final concentration of 5  $\mu$ M in freshly prepared neurobasal medium containing B27 supplements (minus antioxidants) then added to the neuronal cells for 24 h treatment in a 37 °C incubator. Cells were then washed with PBS buffer followed by washing with cold 0.1 M sodium carbonate pH 10 and fixed in 4% paraformaldehyde/PBS for 20 min before being incubated in permeabilization buffer (10% goat serum in PBS containing 0.01% Triton-X) for 20 min and then in blocking buffer (10% goat serum in PBS) for 60 min. Primary anti-Tau antibody (Rabbit polyclonal, Dako, Sydney, Australia) was diluted at 1:1000 in block buffer and incubated on the cells overnight at 4 °C. The cells were washed several times in PBS, and finally incubated in an anti-rabbit-Alexa567 secondary antibody (1:500 in block buffer) and DAPI (for the detection of the cell nucleus) for 60 min, washed in PBS then mounted onto glass slides using mounting media (Prolong Gold, Invitrogen). A Zeiss axioScope2 microscope using a 40X objective lens equipped with a Zeiss HRc camera with filter sets for FITC (green) and Rhodamine (red) was used to take images for histological binding analysis. Identical settings and exposure time were used to capture images for both peptides. The images were processed using Zen blue software (Zeiss, Germany) to generate tiff images before importing them into ImageJ software (NIH, version 1.5b),<sup>28</sup> and the area and integrated density parameter measurements were determined from the selected regions of interest from the images containing neuronal cell structures. The corrected total cell fluorescence intensity = [integrated density – (area of selected cell)  $\times$  (mean fluorescence of background readings)].

## Acknowledgements

The authors thank Dr J. Karas for his advice on peptide synthesis and purification. This work was funded by a grant from the National Health and Medical Research Council of Australia to GDC and seed grant funds from the Melbourne Neuroscience Institute, awarded to GDC, MAH and FS.

## Notes and references

- 1 C. L. Masters and D. J. Selkoe, *Cold Spring Harbor Perspect. Med.*, 2012, 2, a006262.
- 2 H. Braak and E. Braak, *Acta Neurol. Scand., Suppl.*, 1996, 165, 3–12.



- 3 M. P. Kummer and M. T. Heneka, *Alzheimer's Research & Therapy*, 2014, **6**, 1–9.
- 4 S. Kumar, O. Wirths, S. Theil, J. Gerth, T. A. Bayer and J. Walter, *Acta Neuropathol.*, 2013, **125**, 699–709.
- 5 S. Kumar, N. Rezaei-Ghaleh, D. Terwel, D. R. Thal, M. Richard, M. Hoch, J. M. Mc Donald, U. Wullner, K. Glebov, M. T. Heneka, D. M. Walsh, M. Zweckstetter and J. Walter, *EMBO J.*, 2011, **30**, 2255–2265.
- 6 I. A. Popov, M. I. Indeikina, S. I. Pekov, N. L. Starodubtseva, A. S. Kononikhin, M. I. Nikolaeva, E. N. Kukaev, Y. I. Kostyukevich, S. A. Kozin, A. A. Makarov and E. N. Nikolaev, *Mol. Biol.*, 2014, **48**, 607–614.
- 7 S. Kumar and J. Walter, *Aging*, 2011, **3**, 803–812.
- 8 E. L. Ashby, J. S. Miners, S. Kumar, J. Walter, S. Love and P. G. Kehoe, *Neuropathol. Appl. Neurobiol.*, 2015, **41**, 428–444.
- 9 S. Kumar, S. Singh, D. Hinze, M. Josten, H. G. Sahl, M. Siepmann and J. Walter, *J. Biol. Chem.*, 2012, **287**, 8641–8651.
- 10 T. L. Lau, J. D. Gehman, J. D. Wade, C. L. Masters, K. J. Barnham and F. Separovic, *Biochim. Biophys. Acta*, 2007, **1768**, 3135–3144.
- 11 G. D. Ciccotosto, D. J. Tew, S. C. Drew, D. G. Smith, T. Johanssen, V. Lal, T. L. Lau, K. Perez, C. C. Curtain, J. D. Wade, F. Separovic, C. L. Masters, J. P. Smith, K. J. Barnham and R. Cappai, *Neurobiol. Aging*, 2011, **32**, 235–248.
- 12 T. L. Williams and L. C. Serpell, *FEBS J.*, 2011, **278**, 3905–3917.
- 13 A. A. Spector and M. A. Yorek, *J. Lipid Res.*, 1985, **26**, 1015–1035.
- 14 E. Jamasbi, G. D. Ciccotosto, J. Tailhades, R. M. Robins-Browne, C. L. Ugalde, R. A. Sharples, N. Patil, J. D. Wade, M. A. Hossain and F. Separovic, *Biochim. Biophys. Acta*, 2015, **1848**, 2031–2039.
- 15 S. A. Hudson, H. Ecroyd, T. W. Kee and J. A. Carver, *FEBS J.*, 2009, **276**, 5960–5972.
- 16 M. K. Jana, R. Cappai, C. L. Pham and G. D. Ciccotosto, *J. Neurochem.*, 2016, **136**, 594–608.
- 17 G. D. Ciccotosto, D. Tew, C. C. Curtain, D. Smith, D. Carrington, C. L. Masters, A. I. Bush, R. A. Cherny, R. Cappai and K. J. Barnham, *J. Biol. Chem.*, 2004, **279**, 42528–42534.
- 18 B. Bacsá, S. Bosze and C. O. Kappe, *J. Org. Chem.*, 2010, **75**, 2103–2106.
- 19 A. K. Tickler, A. B. Clippingdale and J. D. Wade, *Protein Pept. Lett.*, 2004, **11**, 377–384.
- 20 A. K. Tickler, C. J. Barrow and J. D. Wade, *J. Pept. Sci.*, 2001, **7**, 488–494.
- 21 A. A. Kulikova, P. O. Tsvetkov, M. I. Indeykina, I. A. Popov, S. S. Zhokhov, A. V. Golovin, V. I. Polshakov, S. A. Kozin, E. Nudler and A. A. Makarov, *Mol. BioSyst.*, 2014, **10**, 2590–2596.
- 22 N. Rezaei-Ghaleh, S. Kumar, J. Walter and M. Zweckstetter, *J. Biol. Chem.*, 2016, **291**, 16059–16067.
- 23 N. Rezaei-Ghaleh, M. Amininasab, K. Giller, S. Kumar, A. Stundl, A. Schneider, S. Becker, J. Walter and M. Zweckstetter, *J. Am. Chem. Soc.*, 2014, **136**, 4913–4919.
- 24 N. G. N. Milton, *NeuroReport*, 2001, **12**, 3839–3844.
- 25 M. K. Jana, R. Cappai and G. D. Ciccotosto, *ACS Chem. Neurosci.*, 2016, **7**, 1141–1147.
- 26 D. G. Smith, G. D. Ciccotosto, D. J. Tew, K. Perez, C. C. Curtain, J. F. Boas, C. L. Masters, R. Cappai and K. J. Barnham, *J. Alzheimers Dis.*, 2010, **19**, 1387–1400.
- 27 S. Kumar, O. Wirths, K. Stuber, P. Wunderlich, P. Koch, S. Theil, N. Rezaei-Ghaleh, M. Zweckstetter, T. A. Bayer, O. Brustle, D. R. Thal and J. Walter, *Acta Neuropathol.*, 2016, **131**, 525–537.
- 28 C. A. Schneider, W. S. Rasband and K. W. Eliceiri, *Nat. Methods*, 2012, **9**, 671–675.

